



Saturation spectroscopy of R(0), R(2) and P(2) lines in the (2-0) band of HD

F. M. J. Cozijn¹, M. L. Diouf¹, and W. Ubachs^a

Department of Physics and Astronomy, LaserLab, Vrije Universiteit, De Boelelaan 1081, 1081 Amsterdam, HV, The Netherlands

Received 10 October 2022 / Accepted 7 November 2022 / Published online 18 November 2022
© The Author(s) 2022

Abstract. Lamb-dips of R(0), R(2) and P(2) rovibrational transitions in the (2-0) overtone band of the HD molecule are measured at cryogenic temperatures using the technique of NICE-OHMS spectroscopy. Resulting transition frequencies are 214 905 335 240 (100) kHz for R(0), 219 042 856 794 (150) kHz for R(2) and 206 898 802 150 (150) kHz for P(2). Small, but systematic deviations (at 1.7σ level) are found from advanced ab initio calculations, supporting results from previous studies probing other lines in the (2-0) band. From a combination difference between the R(0) and P(2) lines, an accurate value for rotational-level spacing in the $v = 0$ ground state is determined, of $\Delta_{(J=2)-(J=0)} = 8\,006\,533\,168$ (26) kHz, well in agreement with theory (at 0.6σ). Based on the observation of the dispersive line shape of R(0), the status of proposed models for the elusive line shapes of saturated transitions in HD is discussed.

1 Introduction

Precision spectroscopy of the hydrogen molecule is a favoured avenue for testing molecular quantum electrodynamics and to search for new physics [1]. One of the targets has been the determination of the dissociation energies of various isotopologues, where developments on the experimental side [2–4] and on the theoretical side [5–7] have gone hand in hand in a mutually stimulating fashion. The theoretical development [8] has led to the public availability of a program suite delivering binding energies of all rovibrational states in all hydrogen isotopologues at high accuracy [9].

The vibrational spectroscopy of HD is a another preferred target for precision studies, since the small dipole moment in this heteronuclear species gives stronger absorption strength compared to that in homonuclear species, where only quadrupole transitions are allowed [10]. Cavity-enhanced techniques were employed to perform Doppler-broadened spectroscopies of the (2-0) band at a wavelength of $1.4\ \mu\text{m}$ [11, 12]. Progress in precision was achieved, when saturation spectroscopy of R-lines in the (2-0) overtone band was demonstrated [13, 14]. These studies revealed unexpected asymmetric line shapes for the saturated absorption features that hamper the precision at which transition frequencies can be determined. Thereafter, a number of studies were performed on the dispersive-like line shapes for which various interpretations were postulated, ranging from underlying hyperfine structure and crossover

resonances [15, 16] to a Fano line shape resulting from discrete–continuum interaction in the excitation of HD [17]. Also, effects of the standing waves produced by the strong intracavity laser fields were considered [18].

The R(0) line in the (2-0) band of HD had been inaccessible from spectroscopic studies since it is overlaid with a strong water vapour absorption line. However, in specially designed cryo-cooled intracavity measurement set-ups the R(0) could be measured under Doppler-broadened conditions [19, 20]. In the present study, a cryogenic approach is combined in a noise-immune-cavity-enhanced optical-heterodyne molecular spectroscopy (NICE-OHMS) experiment in which the R(0) transition is saturated and measured under Doppler-free conditions. From similar measurements on the R(2) and P(2) lines, accurate values for rotational-level splittings are determined via combination differences. This work follows the method of a previous study that combined precision measurements of R(1), R(3) and P(3) lines [21].

2 Experiment

The NICE-OHMS set-up at the Amsterdam laboratory is essentially similar to that used in previous experiments on HD [14–16, 21]. The novelty is that the optical cavity is rebuilt and attached to a cryo-cooler to reach temperatures in the range 50–300 K. Details of the cryo-cooled cavity design and operation will be communicated in a forthcoming paper [22]. For the spec-

^a e-mail: w.m.g.ubachs@vu.nl (corresponding author)

troscopy, a diode laser, running at $1.4\ \mu\text{m}$, is used. The laser is locked to the cavity for short-term stability and to a frequency comb laser for long-term stability and for setting the absolute frequency scale. By locking the comb to a Cs-clock, the accuracy of the absolute frequency averages down to below kHz in long-term measurements. Another improvement is in the use of a free-space electro-optic modulator (EOM) with better transmissivity compared to the previously used fibre EOM, now yielding an intracavity circulating power at the central carrier frequency f_c of 450 W. Sidebands are generated at $f_c \pm f_m$ with $f_m = 404\ \text{MHz}$ for generating the NICE-OHMS signal and at $f_{\text{PDH}} = 20\ \text{MHz}$ for the Pound–Drever–Hall cavity lock. In addition, slow wavelength dithering of the cavity length is applied at 395 Hz allowing for lock-in detection. Depending on the dither modulation amplitude, this dithering may induce broadening of the observed spectrum. In the present study, only $1f$ demodulation is applied. In view of the better vibration isolation of the upgraded cavity and suppression of drifting background signal, there is no need to use $2f$ demodulation for further noise removal. For further details, we refer to previous reports [14–16,21].

3 Results

3.1 Vibrational transitions

Results of recorded saturated spectra for the R(0) line in the (2-0) band of HD, measured at temperatures of 57 K and 180 K and for pressures in the range of 0.01–0.5 Pa, are presented in Fig. 1. At these low temperatures, water vapour is completely frozen and indeed the strong (101)₂₁₁-(000)₃₁₂ water line at 214 904 335 MHz does not hinder the recording of R(0). The recorded spectra feature a combination of a ‘Lamb-peak’ at the low-frequency side and a Lamb-dip at the high-frequency side, resulting in a dispersive line shape as discussed before for other saturated lines in the HD (2-0) band [15,17,18,21].

Here, we note again, as in our previous study [21], that generic signals produced in direct NICE-OHMS spectroscopy exhibit a dispersive line shape, as a result of the frequency modulation spectroscopy applied [23,24]. A recording of a spectrum with an additional low-frequency dither modulation to the cavity length, as in the present study, and demodulation at $1f$ by a lock-in amplifier, typically produces a symmetric line shape. This was shown for measurements of Lamb-dips in H₂O [25]. Hence, the present $1f$ demodulated spectra may be compared with results from cavity ring-down or cavity-enhanced spectroscopy. The observations displayed in Fig. 1 demonstrate that the R(0) line, measured in saturation, produces an intrinsically dispersive line shape, similar to the NICE-OHMS observations of R(1), R(3) and P(3) lines [21] as well as the observations in HD from other cavity-enhanced techniques [17].

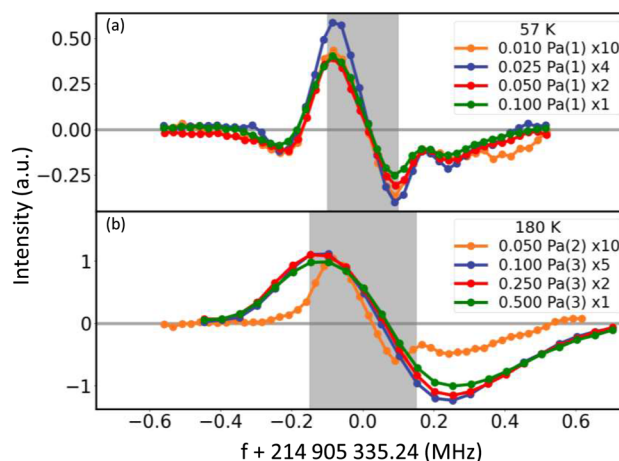


Fig. 1 Spectrum of the R(0) line in the (2-0) overtone band of HD in saturated absorption employing the NICE-OHMS technique in the cryo-cooled set-up using $1f$ demodulation. Spectra were measured at temperatures of 57 K **a** and 180 K **b** for pressures as indicated in the legend. The different indexes represent the broadening due to the dithering effect: (1) 10 kHz, (2) 50 kHz and (3) 200 kHz. The spectra have been scaled to their respective pressures with multiplication factors as indicated. The 0.0 value at the x -axis represents the deduced transition frequency of R(0): 214 905 335.240 (0.100) MHz

The apparent asymmetry and the lack of a fully quantitative model for the observed line shape prohibit the determination of the transition frequency of the rovibrational R(0) line at an accuracy as high as for symmetric water lines [25]. Hence, values for the transition frequency and its uncertainty are estimated by considering that the rovibrational frequency is contained in the most pronounced part of the line shape. The region of this estimate is indicated by the grey bars in Fig. 1. The example of the absorption feature at cryo-temperatures (57 K) gives rise to the narrowest feature, leading to a determination of the transition frequency of R(0) of 214 905 335.240 (0.100) MHz.

The spectra recorded at different pressures provide insight into the collisional shift of the R(0) line. In view of the conservative uncertainty estimate, as indicated by the grey bar, its contribution to the error budget ($< 10\ \text{kHz}$) is much smaller than the uncertainty due to the dispersive line shape. Different modulation amplitudes of dithering have been used throughout this study. For the measurements at 57 K, the smallest dithering amplitude was applied, giving rise to a broadening of 10 kHz. Larger modulation amplitudes have been used for the spectra acquired at 180 K, resulting in broadening effects of 50 kHz and 200 kHz, respectively. Figure 1 clearly illustrates the effect of dithering amplitude, showing a larger impact on the spectral width than the variation of pressure.

Recordings of $1f$ -demodulated NICE-OHMS spectra of R(2) and P(2) lines in the (2-0) band are displayed in Fig. 2. These measurements were performed at a temperature of 180 K. At the 57 K setting, the population

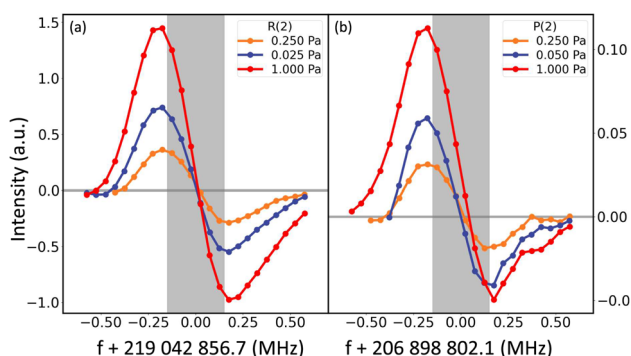


Fig. 2 Spectra of **a** R(2) and **b** P(2) lines in the (2-0) band of HD in saturated absorption employing the NICE-OHMS technique in the cryo-cooled set-up using 1*f* demodulation. Spectra were measured at temperatures of 180 K for pressures as indicated in the legend. The broadening effect induced by the dithering amplitude is estimated at up to 200 kHz

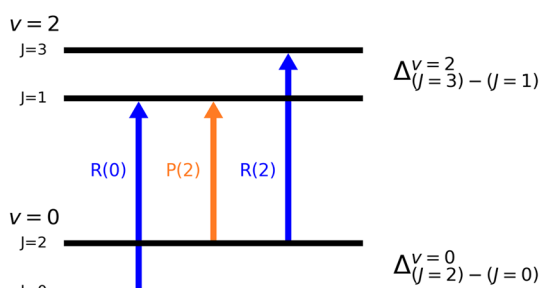


Fig. 3 Level scheme of HD showing how the three lines R(0), R(2) and P(2) correspond to rotational-level spacings in the *v* = 0 ground and *v* = 2 excited vibrational level

in the *J* = 2 ground level was too small for obtaining good quality spectra. Again, an estimate of the uncertainty of the P(2) and R(2) vibrational transition frequencies is made commensurate with the grey bar covering the resonance. In these cases, of broader lines, the uncertainty is estimated at 150 kHz.

3.2 Rotational-level separations

Inspection of Figs. 1 and 2 reveals that the saturation spectra for the three HD resonances as recorded via 1*f*-demodulated NICE-OHMS exhibit asymmetric line shapes that deviate from expected line shapes in NICE-OHMS. However, the dispersion-like line shapes of the R(0), R(2) and P(2) are rather similar to each other as well as to line profiles of the previously investigated R(1), R(3) and P(3) lines [21]. Again combination differences will be used to extract information on rotational-level spacings as illustrated in Fig. 3, in this case the spacings $\Delta_{(J=2)-(J=0)}$ in the ground vibrational *v* = 0 level, and $\Delta_{(J=3)-(J=1)}$ in the *v* = 2 vibrational level.

In Fig. 4, spectra of 1*f*-demodulated spectra for the three HD lines, all recorded at 180 K, are compared. The procedure for comparison is similar as previously

described [21]. Auto-correlation and cross-correlation functions for the pairs R(0)-P(2) and R(2)-P(2) demonstrate quantitatively the similarity between the spectra, with a peak overlap of 85% and 95% for the cross-correlated pairs, respectively. Fitting of standard cubic spline interpolations is employed to produce a functional form closely representing the line shapes of the strong R(0) and R(2) lines as shown in panels (e) and (f). These resulting functional forms are then used to fit the weak P(2) line in both cases. In this final step, a frequency shift term Δ is determined, delivering frequency shifts between the R(0)/P(2) and R(2)/P(2) pairs. This procedure results in combination differences between the line pairs, and therewith rotational-level spacings $\Delta_{(J=2)-(J=0)}^{v=0}$ and $\Delta_{(J=3)-(J=1)}^{v=2}$ at a statistical accuracy of 12 kHz and 5 kHz, respectively.

Underlying hyperfine structure of the resonance lines may cause a systematic effect on the determination of the combination differences. The hyperfine structure of all three lines is evaluated based on the computations of Ref. [26]. Computed intensities of individual hyperfine components are convolved with a 1*f* derivative of a dispersive line shape function to produce a width commensurate with the width (Γ = 700 kHz FWHM) obtained in the spectra observed at 180 K. This allows for a computation of the shift of line centre from the centre of gravity of the hyperfine structure, resulting in shifts of 0 kHz, 0 kHz and +10 kHz for the R(0), R(2) and P(2) lines, respectively. The shifts for the P(2) line are included in the error budget for the pure rotational line spacings.

The shift due to the pressure is systematically investigated in Fig. 5. Using a linear regression, the pressure-free position has been extracted as well as the slopes for the individual rotational-level spacings. The pressure shift slopes have been estimated at -18.5 (28) kHz/Pa for the R(0)/P(2) pair and -19.8 (2) kHz for R(2)/P(2) pair, while the extracted uncertainties of 22 kHz and 2 kHz have been included in the error budget.

Taking all uncertainty contributions into account values for the rotational-level spacings are determined for $\Delta_{(J=2)-(J=0)}^{v=0} = S^0(0) = 8\,006\,533\,168(26)$ kHz and $\Delta_{(J=3)-(J=1)}^{v=2} = S^2(1) = 12\,144\,054\,660(20)$ kHz.

4 Discussion

4.1 Comparison with QED calculations

The present results for the vibrational transition frequencies of the R(0), R(2) and P(2) in the (2-0) overtone band of HD, as obtained via NICE-OHMS saturation spectroscopy, are listed in Table 1 with all previously obtained precision measurements for this band. The content of Table 1 is limited to experimental values for which the precision exceeds that of quantum electrodynamic (QED) calculations from the H2SPECTRE program (version 7.3) [9] with neglect of older less precise data [21].

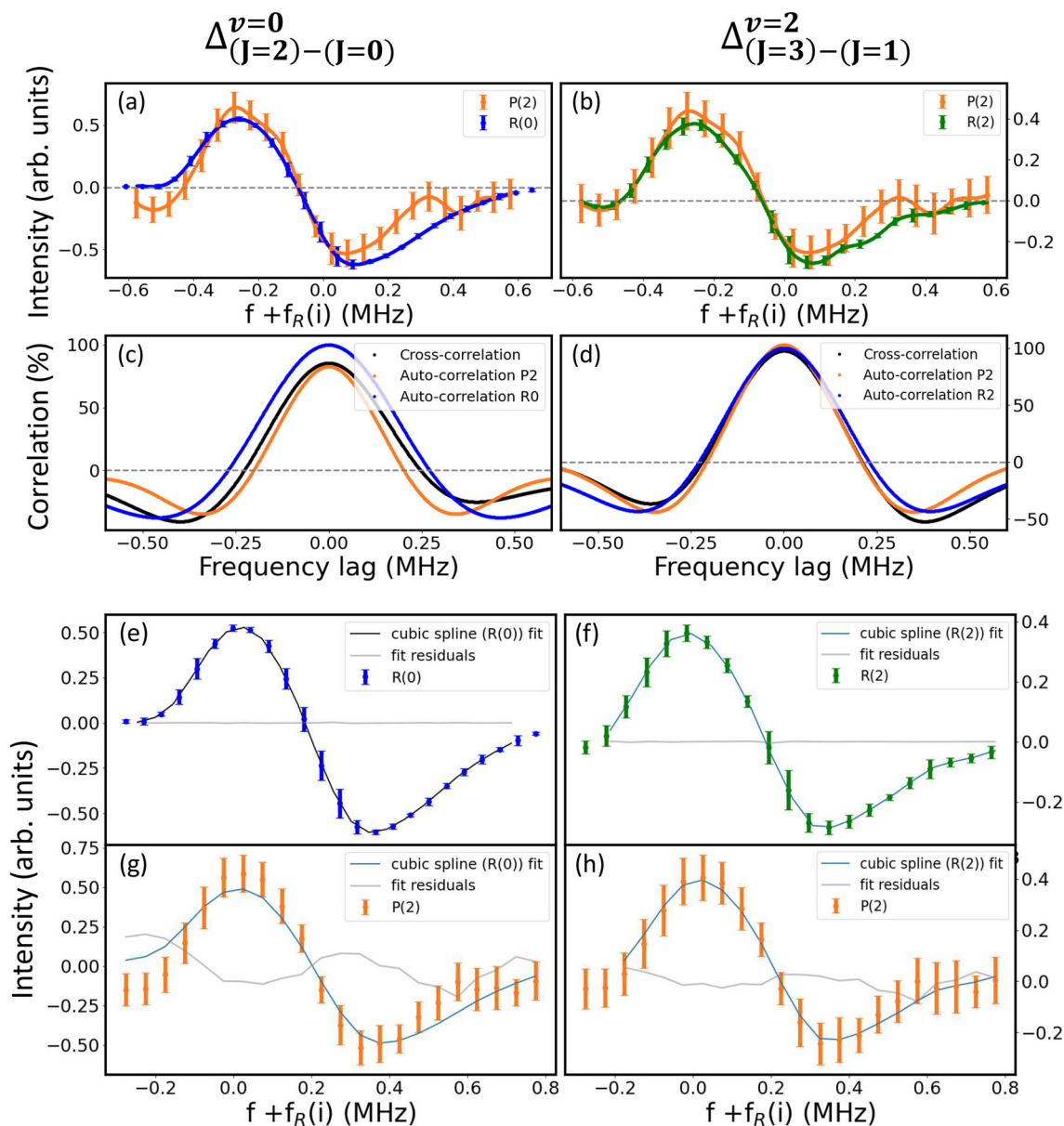


Fig. 4 Analysis of combination differences from comparison of the saturation spectra for three HD lines in the (2-0) overtone band, all recorded at a pressure of 0.25 Pa, temperature of 180 K, and at 1f demodulation of the NICE-OHMS signal. **a** Comparison for the pair R(0) and P(2). **b** Comparison for the pair R(2) and P(2). Note that the amplitudes for the corresponding spectra are adapted to match each other. **c** Results of auto-correlation and cross-correlation calculations for the R(0)-P(2) pair and **d** for the R(2)-P(2) pair. In panels **e** and **f**, fits are made using a cubic spline interpolation for which residuals are computed and plotted (thin grey line). The resulting cubic spline functional form is then fitted to the line shapes of the P(2) lines in **g** and **h**. Residuals of the latter are again plotted in grey

The present frequency determinations corroborate the findings discussed in the study on R(1), R(3) and P(3) lines [21], as well as the recent very precise measurement of the R(0) transition under Doppler-broadened and cryo-cooled conditions [20]. For the present and all previous precision measurements on lines in the (2-0) band, the experimentally determined frequencies are consistently higher than theory by 1.9 ± 0.1 MHz, corresponding to 1.7σ . This further strengthens the indication that the ab initio calculations of

H2SPECTRE (version 7.3) systematically underestimate the vibrational frequencies in HD, even though these calculations are only accurate to 1.1 MHz.

The results on pure rotational transitions and the measurements of rotational-level splittings are compiled in Table 2. Again only the results for which the experimental accuracy exceeds that of the theory are included. There is only a single experimental result for a pure rotational transition, that of the R(0) line [27], performed at a similar accuracy as that of the-

Table 1 Comparison between experimental data, from the present work and literature, and computed results using H2SPECTRE [9] for rovibrational transition frequencies in the (2-0) band of HD with results

Band	Line	Exp. (MHz)	Ref.	H2SPECTRE (MHz)	Diff. (MHz)	Diff. (σ)	
(2-0)	P(1)	209 784 242.007 (0.020)	[16]	209 784 240.1 (1.0)	1.9 (1.1)	1.7	
	P(2)	206 898 802.150 (0.150)	Present	206 898 800.2 (1.0)	1.9 (1.1)	1.8	
	P(3)	203 821 936.805 (0.060)	[21]	203 821 935.0 (1.0)	1.8 (1.0)	1.8	
	R(0)	214 905 335.220 (0.020)	[20]	214 905 333.3 (1.1)	1.9 (1.1)	1.7	
		214 905 335.240 (0.100)	Present	214 905 333.3 (1.1)	1.9 (1.1)	1.7	
		R(1)	217 105 181.901 (0.050)	[15]	217 105 180.0 (1.1)	1.9 (1.1)	1.7
	R(1)	217 105 182.111 (0.240)	[17]	217 105 180.0 (1.1)	2.1 (1.1)	1.9	
		217 105 181.901 (0.076)	[12]	217 105 180.0 (1.1)	1.9 (1.1)	1.7	
		217 105 181.934 (0.020)	[20]	217 105 180.0 (1.1)	1.9 (1.1)	1.7	
		R(2)	219 042 856.621 (0.025)	[14] ^a	219 042 854.7 (1.1)	1.9 (1.1)	1.7
		219 042 856.794 (0.150)	Present	219 042 854.7 (1.1)	2.1 (1.1)	1.9	
	R(3)	220 704 304.951 (0.028)	[14] ^a	220 704 303.0 (1.1)	1.9 (1.1)	1.7	
		220 704 304.984 (0.065)	[21]	220 704 303.0 (1.1)	1.9 (1.1)	1.7	

All frequencies given in MHz. Differences are presented in terms of MHz and in terms of the combined standard deviation (σ) of experiment and theory

^a Results from fitting centre frequency of a Lamb-dip without considering the complex line shape, leading to an underestimate of the uncertainty

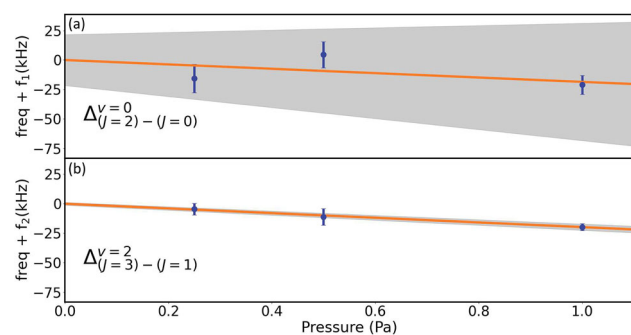


Fig. 5 Pressure effect on the rotational splitting. **a** Effect on S(0) in the $v = 0$ ground state; **b** S(1) in $v = 2$. The shaded grey areas represent the uncertainties of a linear regression fit used. The extracted slopes represent the pressure coefficients with their respective uncertainties yielding **a** -18.5 (28) kHz/Pa and **b** -19.8 (2) kHz/Pa. The pressure-free values have also been extracted with uncertainties of 22 kHz **a** and 2 kHz **b**, respectively

ory. The present measurement of the S(0)-level spacing and that of the previous S(1) separation [21] are somewhat more accurate than theory. Focusing on the $v = 0$ ground level of HD, there are now three accurate experimental data points for comparison with theory. On average, experiment and theory are in agreement within 1σ although the experimental values are consistently at higher frequencies than the theoretical ones. These results provide a challenge for future calculations of HD-level energies, beyond the state of the art of H2SPECTRE version 7.3, which is limited by the computation of the $E^{(5)}$ term in the QED expansion [8, 28, 29].

4.2 Dispersive line shape of R(0)

A discussion has arisen in the literature on the observed line shapes of vibrational transitions in the (2-0) band of HD as measured in saturation after the first reports in 2018 [13, 14]. The observation of asymmetric line shapes, for which no fully quantitative model is yet formulated, hinders the determination of a very accurate frequency. In principle, transition frequencies can be determined to sub-kHz precision in case of unproblematic line shapes, therewith fully exploiting the capabilities of frequency-comb-locked saturation spectroscopy, as was shown for the example of CO₂ [30, 31].

Various models have been proposed for the dispersive nature of the line shapes of saturated lines as observed in HD. The Amsterdam group proposed a model based on the effect of underlying hyperfine structure and the associated crossover resonances. A computation of the line shape with optical Bloch equations (OBE) yielded a good representation for the R(1) line [15]. In this approach, parameters for collisional deexcitation and coherence dephasing were included in the model by fitting to the observed line shape. This model generally predicts a dispersive-like line shape for all transitions in the (2-0) band of HD except for the cases of the P(1) and R(0) lines, where the level scheme is such that either the hyperfine components in the excited state or in the ground state are very close to degeneracy. Note that for $J = 0$ levels in HD hyperfine doublets are of order 50 Hz [32]. In the case of the P(1) line, the OBE model predicts a pure Lamb-peak as was indeed observed in experiment [16]. The OBE model predicts a symmetric pure Lamb-dip for the R(0) resonance. Inspection of Fig. 1 reveals that the saturated absorption spectrum of the R(0) line exhibits a dispersion-like line shape, in contradiction with that prediction.

Table 2 Comparison between experimental precision data and computed results using H2SPECTRE [9] for rotational transition frequencies and level splittings in the $v = 0$ ground level of HD

Band	Line	Exp. (MHz)	Ref.	H2SPECTRE (MHz)	Diff. (MHz)	Diff. (σ)
(0-0)	R(0)	2 674 986.094 (0.025)	[27]	2 674 986.071 (0.022)	0.023 (0.033)	0.7
	S(0) ^a	8 006 533.168 (0.026)	Present	8 006 533.126 (0.066)	0.042 (0.070)	0.6
	S(1) ^a	13 283 245.098 (0.030)	[21]	13 283 244.944 (0.110)	0.158 (0.114)	1.4
(2-2)	S(1) ^a	12 144 054.660 (0.020)	Present	12 144 054.520 (0.099)	0.140 (0.101)	1.4
	S(2) ^a	16 882 368.179 (0.020)	[21]	16 882 367.976 (0.140)	0.200 (0.141)	1.5

All frequencies given in MHz. Differences are presented in terms of MHz and in terms of the combined standard deviation (σ) of experiment and theory

^a Derived from a combination difference

The Hefei group proposed a model identifying the observed profile of the R(1) line as a Fano line shape [17] representative of an interference between a transition to a discrete and a continuum level. The discrete resonance would then be represented by the weak vibrational transition in the (2-0) band, while the continuum would be represented by the Lorentzian tail of the $B^1\Sigma_u^+ - X^1\Sigma_g^+$ electronic band system. This proposal would, however, also predict a similar Fano-type interference for the P(1) line, where it was not observed [16]. In addition, this mechanism should also apply to the case of the measurement of the R(0) line in the (1-0) band measured in a molecular beam [33] as well as in the observations of the R(0) line in the (2-0) band under conditions of cryo-cooling and reduced Doppler width [19,20]. These examples are seemingly in contradiction to the Fano interference mechanism producing dispersive line shapes in HD.

More recently, the Hefei group proposed a mechanism based on the standing wave produced inside the cavity from the strong circulating laser power, affecting the resonant molecules in the interaction path [18]. Spectra of two transitions of $^{13}\text{C}^{16}\text{O}_2$ were recorded in saturation. Whereas a relatively strong line with an Einstein coefficient of $A = 7 \times 10^{-4} \text{ s}^{-1}$ exhibits a symmetric line profile, a much weaker line with $A = 2 \times 10^{-5} \text{ s}^{-1}$ gives rise to a dispersive line shape [18,34]. This is indicative of the fact that the distortion of the line shape, from symmetric to dispersion-like, sets in for very weak lines. Indeed for the R-lines in the (2-0) band of HD an Einstein coefficient of $A = 2.5 \times 10^{-5} \text{ s}^{-1}$ was measured [11], of similar magnitude as for the weakest of the two $^{13}\text{CO}_2$ lines.

In our laboratory, we have observed a similar dispersive line shape for a line of $^{12}\text{C}^{16}\text{O}_2$. The spectrum shown in Fig. 6 represents the R(14e) line in the vibrational band $(4\ 0\ 0\ 15) \leftarrow (0\ 0\ 0\ 01)$ [35]. At an Einstein coefficient of $A = 6 \times 10^{-6} \text{ s}^{-1}$, this is the molecular absorption line with the smallest transition moment ever detected in saturation spectroscopy. Of relevance for the present discussion is that $^{12}\text{C}^{16}\text{O}_2$ has no hyperfine substructure, so the dispersive line shape is observed for a species without underlying substructure. An additional peculiarity of this spectrum is that the

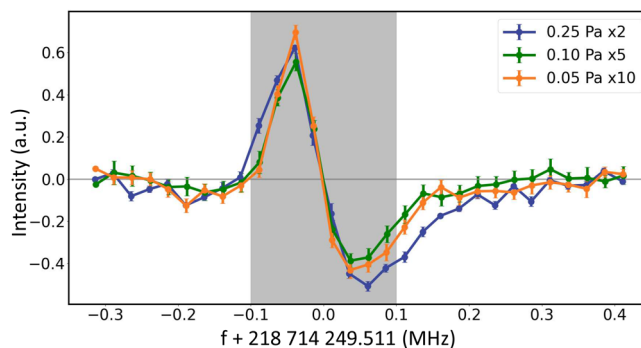


Fig. 6 Spectrum of the R(14e) line in the band $(4\ 0\ 0\ 15) \leftarrow (0\ 0\ 0\ 01)$ of $^{12}\text{C}^{16}\text{O}_2$ measured in saturated absorption employing the NICE-OHMS technique using $1f$ demodulation. The spectra were recorded at 180 K for pressures as indicated in the legend. The broadening effect due to the dithering amplitude amounted to 20 kHz. The spectra have been scaled to their respective pressures with multiplication factors as indicated. The 0.0 value represents a frequency of 218 714 249 511 (100) kHz, deduced in the present study

observed linewidth is much narrower than the transit-time broadening of 290 kHz FWHM at 180 K.

5 Conclusion

The present experimental study reports accurate results for transition frequencies of the R(0), R(2) and P(2) lines in the (2-0) band of HD. The obtained accuracies face a limitation due to the fact that asymmetric line shapes are observed for which no quantitative model exists, so the potential accuracy of frequency-comb-locked saturation spectroscopy could not be exploited. The findings nevertheless support earlier conclusions that the advanced fully ab initio calculations from version 7.3 of the H2SPECTRE program [9] deviate in a systematic fashion from experiment. Combination differences between observed vibrational frequencies can be translated into rotational-level spacings in the $v = 0$ and $v = 2$ vibrational levels of HD at an accuracy better

than for most direct measurement in purely rotational spectroscopy.

The observation of a dispersive line shape for the $R(0)$ line contradicts the expectation of a predicted symmetric Lamb-dip for that line from a model based in which the asymmetry is considered as resulting from underlying hyperfine structure and crossover resonances. Alternative models as presented in the literature are discussed. A quantitative model is, however, not yet developed. Therewith, a full and quantitative explanation of the line shape of saturated molecular transitions under high-power intracavity conditions remains a challenge for precision spectroscopy.

Acknowledgements Financial support from the Netherlands Organisation for Scientific Research, via the Program ‘The Mysterious Size of the Proton’, is gratefully acknowledged.

Author contributions

FMJC designed and built the cryo-cooled cell for the intracavity measurements that were carried out jointly by FMJC and MLD. MLD took the lead in the analysis, and WU wrote a draft for the manuscript that was reviewed by all authors.

Data Availability Statement This manuscript has no associated data or the data will not be deposited. [Authors’ comment: The datasets generated during and/or analysed during the current study are available from the corresponding author on reasonable request.]

Open Access This article is licensed under a Creative Commons Attribution 4.0 International License, which permits use, sharing, adaptation, distribution and reproduction in any medium or format, as long as you give appropriate credit to the original author(s) and the source, provide a link to the Creative Commons licence, and indicate if changes were made. The images or other third party material in this article are included in the article’s Creative Commons licence, unless indicated otherwise in a credit line to the material. If material is not included in the article’s Creative Commons licence and your intended use is not permitted by statutory regulation or exceeds the permitted use, you will need to obtain permission directly from the copyright holder. To view a copy of this licence, visit <http://creativecommons.org/licenses/by/4.0/>.

References

1. W. Ubachs, J.C.J. Koelemeij, K.S.E. Eikema, E.J. Salumbides, Physics beyond the Standard Model from hydrogen spectroscopy. *J. Mol. Spectrosc.* **320**, 1 (2016)
2. J. Liu, E.J. Salumbides, U. Hollenstein, J.C.J. Koelemeij, K.S.E. Eikema, W. Ubachs, F. Merkt, Determination of the ionization and dissociation energies of the hydrogen molecule. *J. Mol. Spectrosc.* **130**, 174306 (2009)
3. N. Hölsch, M. Beyer, E.J. Salumbides, K.S.E. Eikema, W. Ubachs, C. Jungen, F. Merkt, Benchmarking theory with an improved measurement of the ionization and dissociation energies of H_2 . *Phys. Rev. Lett.* **122**, 103002 (2019)
4. J. Hussels, N. Hölsch, C.-F. Cheng, E.J. Salumbides, H.L. Bethlem, K.S.E. Eikema, C. Jungen, M. Beyer, F. Merkt, W. Ubachs, Improved ionization and dissociation energies of the deuterium molecule. *Phys. Rev. A* **105**, 022820 (2022)
5. K. Piszczatowski, G. Łach, M. Przybytek, J. Komasa, K. Pachucki, B. Jeziorski, Theoretical determination of the dissociation energy of molecular hydrogen. *J. Chem. Theory Comput.* **5**, 3039 (2009)
6. M. Puchalski, J. Komasa, P. Czachorowski, K. Pachucki, Nonadiabatic QED correction to the dissociation energy of the hydrogen molecule. *Phys. Rev. Lett.* **122**, 103003 (2019)
7. M. Puchalski, J. Komasa, A. Spyszkiwicz, K. Pachucki, Dissociation energy of molecular hydrogen isotopologues. *Phys. Rev. A* **100**, 020503 (2019)
8. P. Czachorowski, M. Puchalski, J. Komasa, K. Pachucki, Nonadiabatic relativistic correction in H_2 , D_2 , and HD . *Phys. Rev. A* **98**, 052506 (2018)
9. H2SPECTRE ver 7.3 Fortran source code, University of Warsaw, Poland (2019)
10. G. Herzberg, Rotation-vibration spectrum of the HD molecule. *Nature* **166**, 563 (1950)
11. S. Kassı and A. Campargue, Electric quadrupole and dipole transitions of the first overtone band of HD by CRDS between 1.45 and 1.33 μm . *J. Mol. Spectrosc.* **267**, 36 (2011)
12. A. Castrillo, E. Fasci, and L. Gianfrani, Doppler-limited precision spectroscopy of HD at 1.4 μm : An improved determination of the $R(1)$ center frequency. *Phys. Rev. A* **103**, 022828 (2021)
13. L.-G. Tao, A.-W. Liu, K. Pachucki, J. Komasa, Y.R. Sun, J. Wang, S.-M. Hu, Toward a determination of the proton–electron mass ratio from the lamb-dip measurement of HD . *Phys. Rev. Lett.* **120**, 153001 (2018)
14. F.M.J. Cozijn, P. Dupré, E.J. Salumbides, K.S.E. Eikema, W. Ubachs, Sub-Doppler frequency metrology in HD for tests of fundamental physics. *Phys. Rev. Lett.* **120**, 153002 (2018)
15. M.L. Diouf, F.M.J. Cozijn, B. Darquié, E.J. Salumbides, W. Ubachs, Lamb-dips and Lamb-peaks in the saturation spectrum of HD . *Opt. Lett.* **44**, 4733 (2019)
16. M.L. Diouf, F.M.J. Cozijn, K.-F. Lai, E.J. Salumbides, W. Ubachs, Lamb-peak spectrum of the HD (2-0) $P(1)$ line. *Phys. Rev. Res.* **2**, 023209 (2020)
17. T.-P. Hua, Y.R. Sun, S.-M. Hu, Dispersion-like lineshape observed in cavity-enhanced saturation spectroscopy of HD at 1.4 μm . *Opt. Lett.* **45**, 4863 (2020)
18. Y.N. Lv, A.W. Liu, Y. Tan, C.L. Hu, T.P. Hua, X.B. Zou, Y.R. Sun, C.L. Zou, G.C. Guo, S.M. Hu, Nonlinear Fano resonance without a continuum. *Phys. Rev. Lett.* **129**, 163201 (2022)
19. H. Wu, N. Stolarczyk, Q.-H. Liu, C.-F. Cheng, T.-P. Hua, Y.R. Sun, S.-M. Hu, Comb-locked cavity ring-down spectroscopy with variable temperature. *Opt. Express* **27**, 37559 (2019)

20. S. Kassi, C. Lauzin, J. Chaillot, A. Campargue, The (2–0) R(0) and R(1) transition frequencies of HD determined to a 10^{-10} relative accuracy by Doppler spectroscopy at 80 K. *Phys. Chem. Chem. Phys.* **24**, 23164 (2022)
21. F.M.J. Cozijn, M.L. Diouf, V. Hermann, E.J. Salumbides, M. Schlösser, W. Ubachs, Rotational level spacings in HD from vibrational saturation spectroscopy. *Phys. Rev. A* **105**, 062823 (2022)
22. F.M.J. Cozijn et al., to be published
23. A. Foltynowicz, F. Schmidt, W. Ma, O. Axner, Noise-immune cavity-enhanced optical heterodyne molecular spectroscopy: current status and future potential. *Appl. Phys. B* **92**, 313 (2008)
24. O. Axner, W. Ma, A. Foltynowicz, Sub-Doppler dispersion and noise-immune cavity-enhanced optical heterodyne molecular spectroscopy revised. *J. Opt. Soc. Am. B* **25**, 1166 (2008)
25. R. Tobias, T. Furtenbacher, I. Semko, A.G. Csazar, M.L. Diouf, F.M.J. Cozijn, J.M. Staa, E.J. Salumbides, W. Ubachs, Spectroscopic-network-assisted precision spectroscopy and its application to water. *Nature Commun.* **11**, 1709 (2020)
26. H. Jóźwiak, H. Cybulski, P. Wcisło, Positions and intensities of hyperfine components of all rovibrational dipole lines in the HD molecule. *J. Quant. Spectr. Rad. Transfer* **253**, 107171 (2020)
27. B.J. Drouin, S. Yu, J.C. Pearson, H. Gupta, Terahertz spectroscopy for space applications: 2.5–2.7 THz spectra of HD, H₂O and NH₃. *J. Mol. Struct.* **1006**, 2 (2011)
28. M. Puchalski, J. Komasa, P. Czachorowski, K. Pachucki, Complete α^6m corrections to the ground state of H₂. *Phys. Rev. Lett.* **117**, 263002 (2016)
29. J. Komasa, M. Puchalski, P. Czachorowski, G. Lach, K. Pachucki, Rovibrational energy levels of the hydrogen molecule through nonadiabatic perturbation theory. *Phys. Rev. A* **100**, 032519 (2019)
30. K. Bielska, A. Cygan, M. Konefał, G. Kowzan, M. Zaborowski, D. Charczun, S. Wójtewicz, P. Wcisło, P. Masłowski, R. Ciuryło, D. Lisak, Frequency-based dispersion Lamb-dip spectroscopy in a high finesse optical cavity. *Opt. Express* **29**, 39449 (2021)
31. Y. Tan, Y.R. Xu, T.P. Hua, A.W. Liu, J. Wang, Y.R. Sun, S.M. Hu, Cavity-enhanced saturated absorption spectroscopy of the (30012) - (00001) band of ¹²C¹⁶O₂. *J. Chem. Phys.* **156**, 044201 (2022)
32. M. Puchalski, J. Komasa, K. Pachucki, Hyperfine structure of the first rotational level in H₂, D₂ and HD molecules and the deuteron quadrupole moment. *Phys. Rev. Lett.* **125**, 253001 (2020)
33. A. Fast, S.A. Meek, Sub-ppb measurement of a fundamental band rovibrational transition in HD. *Phys. Rev. Lett.* **125**, 023001 (2020)
34. S.-M. Hu, Precise lineshape parameters from Doppler-free spectroscopy at low pressures, in 25th International Conference on Spectral Line Shapes, Caserta, Italy, 19–24 June (2022)
35. B. Perevalov, V. Perevalov, A. Campargue, A (nearly) complete experimental linelist for ¹³C¹⁶O₂, ¹⁶O¹³C¹⁸O, ¹⁶O¹³C¹⁷O, ¹³C¹⁸O₂ and ¹⁷O¹³C¹⁸O by high-sensitivity CW-CRDS spectroscopy between 5851 and 7045 cm⁻¹. *J. Quant. Spectr. Rad. Transfer* **109**, 2437 (2008)